



OPEN Atorvastatin negatively regulates MAPK pathway in vitro to inhibit proliferation, migration, and invasion of hepatocellular carcinoma cells

Yuhua Meng^{1,7}, Linfang Mo^{2,3,7}, Tianyi Liang^{4,7}, Shutian Mo⁵, Chuangye Han⁵✉ & Yongfei He^{5,6}✉

Hepatocellular carcinoma (HCC) is a prevalent type of tumor. Given the controversy surrounding atorvastatin and HCC, we conducted this study to determine whether atorvastatin has anticancer activity against HCC. The impact of varying concentrations of atorvastatin (ATO) on the biological function of HCC cells was studied in vitro, high-throughput mRNA assays on cells and tumor tissue. Finally, an examination was conducted to assess the correlation between the ATO and the prognosis of HCC. ATO significantly inhibited the proliferation, migration, and invasiveness of HCC cells. Furthermore, in vivo, animal experiments showed that a high-fat diet facilitated the progression of HCC and that ATO did not effectively counteract these detrimental consequences. Tumor sequencing of cells and normal diet mice revealed the disparities were primarily concentrated in the MAPK signaling pathway. Western blot demonstrated ATO reduced the expression of levels of p-MEK, p-RAF1, p-P38, p-ERK, and p-JNK proteins in HCC cells compared to controls. Clinical data showed that HCC patients with ATO exhibited improved recurrence-free survival (RFS) and overall survival (OS). Following the utilization of propensity score, HCC patients with ATO were found to have better OS, whereas there was no substantial difference in RFS. Atorvastatin effectively inhibits the proliferation, invasion, and migration of HCC cells in vitro through the MAPK pathway. Additionally, ATO may help improve the prognosis of some individuals with HCC.

Keywords Atorvastatin, Hepatocellular carcinoma, MAPK pathway, Proliferation, Prognosis

The World Health Organization estimates that 830,000 people will die from hepatocellular carcinoma by 2020, making it the third highest cause of mortality associated tumors. HCC and cholangiocarcinoma are the main subtypes of primary liver cancer, and HCC accounts for more than 80% of them¹. By 2020, one million new cases of HCC will be diagnosed². China is experiencing an increase in the incidence of HCC, mainly due to a growing aging population, viral hepatitis, and changing dietary habits. The high incidence and mortality rate of HCC have caused significant health problems for our people and a significant economic burden. HCC is closely associated with altered lipid intake, intestinal flora disorders, viral hepatitis, and genetic changes³⁻⁶. Depending on the tumor's stage, HCC treated methods including surgical resection, radiofrequency ablation,

¹School of Medicine, Jinan University, Guangzhou, Guangdong Province, People's Republic of China. ²Department of Nuclear Medicine, The Affiliated Hospital of Youjiang Medical University for Nationalities, Baise, People's Republic of China. ³Key Laboratory of Research on Clinical Molecular Diagnosis for High Incidence Diseases in Western Guangxi of Guangxi Higher Education Institutions, Baise, Guangxi Zhuang Autonomous Region, People's Republic of China. ⁴Department of Hepatobiliary Surgery, The Second Affiliated Hospital of Guangxi Medical University, Nanning, Guangxi Zhuang Autonomous Region, People's Republic of China. ⁵Department of Hepatobiliary Surgery, The First Affiliated Hospital of Guangxi Medical University, Nanning, Guangxi Zhuang Autonomous Region, People's Republic of China. ⁶Department of Hepatopancreatobiliary Surgery, The Eighth Affiliated Hospital of Sun Yat-sen University, Shenzhen, People's Republic of China. ⁷Yuhua Meng, Linfang Mo and Tianyi Liang have contributed equally to this work and share first authorship. ✉email: hanchuangye@hotmail.com; hyf20190701@163.com

chemotherapy, liver transplantation, targeted therapy, immunotherapy^{7–9}. However, no curative treatment has been achieved for advanced HCC, and overall survival remains unsatisfactory. Hence, it is of imperative to conduct additional investigation into the developmental mechanism of HCC and explore the clinical use of complementary therapies. A study of tumor nutrients revealed that lipid metabolism acts as a critical regulator in the tumors developing, along with sugar and amino acids¹⁰. The body contains a variety of lipids, including triglycerides, cholesterol, and lipids. It has been demonstrated that Lipoproteins are crucial for the development of several cancers, including pancreatic, breast, prostate, and others^{11–13}. Studies on lipids have concentrated on triglycerides and cholesterol in different cancers, and their roles in different cancers differ significantly. The liver synthesizes and metabolizes most of the body's lipids, since it is the body's largest metabolic and material synthesis organ. There is evidence that disorders of cholesterol metabolism contribute to liver cancer development^{14–16}. In contrast, the molecular mechanisms of cholesterol's effect on HCC have not been fully explored.

Statins are the most prescribed cholesterol-lowering drugs. Several previous studies have revealed that statins reduce cancer-related deaths and hepatocarcinogenesis^{17–19}. Few studies have examined the molecular signaling pathways associated with statins. The inhibitory effect of atorvastatin on HCC cell proliferation has been shown to be mediated through the IL-6/STAT3 signaling pathway²⁰. A recent study revealed that a high-cholesterol diet leading to the fatty liver-related HCC developing. Under the influence of a high-fat diet, ATO inhibited cholesterol synthesis, which reversed the proliferation of HCC cells¹⁵. Despite this, the study by Zhang X et al. has not yet addressed the molecular pathways that promote HCC development and inhibit it by atorvastatin under high-fat conditions¹⁵. While the role of statins and lipid metabolism in HCC has been explored, the specific interaction between atorvastatin, dietary lipids, and the MAPK pathway in modulating HCC progression remains less defined. This study aims to integrate *in vitro*, *in vivo*, and clinical retrospective analyses to investigate this interplay, providing a more comprehensive understanding of atorvastatin's potential effects in the context of different metabolic environments. Through *in vivo/ex vivo* experiments, this paper explores the effects of atorvastatin and a high-fat diet on molecular signaling pathways in hepatocellular carcinoma, which might lead to improvements in quality of life and an extended lifespan of hepatocellular carcinoma patients.

Materials and methods

Materials

The MHCC-97H (item No. :iCell-h143) cell line was purchased from Cybikang, and the Huh7 (item No.: CL-0120) cell line was purchased from PriCells Life Science and Technology Co., Ltd. in Wuhan. Cells were cultured in DMEM medium with 10% fetal bovine serum (GIBCO, New York, NY, USA), 100 units/mL penicillin G, and 100 µg/mL streptomycin (Solarbio, Beijing, China) added. The cells were then incubated at 37 °C in an incubator with 5% CO₂.

Cell proliferation analysis

The cellular proliferation ability was assessed using the CCK8 test. 100 µL of medium containing 5 × 10³ cells were placed into each well of a 96-well plate overnight. Subsequently, different concentrations of ATO were added. Following incubation period of 24 h and 48 h, CCK8 (Biosharp, China) was introduced and subsequently cultured in the incubator for 2 h. The absorbance values at 450 nm were measured using an enzyme marker (Thermo, UK), and the cell inhibition rate and the half inhibition concentration (IC₅₀) were calculated. Then they were categorized into our groups based on their IC₅₀: a low (L), a medium (M) and a high (H) concentration groups and a blank control group (CK).

Cell cycle assay

To digest Huh7 and MHCC97-H cells, 1 mL of medium containing 3.5 × 10⁵ cells was introduced to each well of a 6-well plate. The plate was then incubated in an incubator at 37 °C and 5% CO₂ for 24 h. The cells were incubated for 24 h by adding the corresponding concentration of sub-Ato according to the above grouping. Subsequently, they were collected and fixed with 70% ethanol at 4 °C for 24 h. The cells were rinsed with phosphate buffered saline (PBS) to remove ethanol stained in accordance with the cell cycle assay kit (Beyotime, China). The cell cycle distribution was used to detect by flow cytometry for 30 min at 25 °C and keep in dark place.

Migration and invasion analysis

Matrigel (285 µg/mL, Corning) diluted in serum-free medium (SFM) was introduced to chamber (8 µm pore size, BD) and were incubated for 120 min at 37 °C to gelate. For migration experiments, pretreatment of Transwell chambers is not required. The cells were subjected to ATO for 1 day are then collected and counted by resuspension in SFM. And we added 300 µL SFM consists of 1.0 × 10⁵ cells to the upper chamber. Meanwhile, 700 µL medium containing 10% FBS was supplemented to the 24-well plate in which the transwell chambers were placed. After 48 h of incubation, we removed the cells in upper by PBS, fixed by paraformaldehyde, and stain with crystal violet after fixing. Five fields of view were randomly selected under an inverted microscope (×200) to calculate the cell volume.

Animal model establishment and management

A total of Twenty male BALB/C nude (BALB/c-nu/nu) mice, aged 4 weeks, with an average weight of 20 ± 2 g, and free of specific pathogens (SPF) were acquired from the Medical Animal Experiment Center of Guangxi Medical University. The mice were categorized into four groups: A, B, C, and D by random number method. After one week of feeding on a normal diet (protein, carbohydrate and fat, nutrient function ratios of 23.07%, 65.08% and 11.85%, respectively; 1010088, Cooperative biology), the feces of each group were collected. Subsequently, the diet of mice in groups C and D was adjusted to special high-fat diet (protein, carbohydrate and fat, nutrient function ratios of 20%, 20%, and 60%, respectively; D12492, BIOFIVEN). After continued feeding

for one week, 1.0×10^6 MHCC97-H cells were injected subcutaneously into the mice. Tumor growth was then evaluated every other day, and drug intervention was started once the average tumor volume reached roughly 100 mm^3 . Mice in groups B and D were injected intraperitoneally according to $40 \mu\text{g/g}$ body weight, and drug treatment was administered every other day five consecutive times. Tumor volume was measured every other day. Under deep anesthesia induced by an intraperitoneal injection of pentobarbital sodium (100 mg/kg), the mice were euthanized via cervical dislocation. This procedure was carried out 14 days after the cessation of drug treatment. Subsequently, blood samples were collected from the mice for biochemical index testing. Some of the tumor tissues underwent high-throughput sequencing of their mRNA, while the remaining tumor tissues were embedded in paraffin.

Detection of cytokines in serum

The levels of cytokines (IL-10, IL-22, and IL-23) was performed via ELISA kits with serum samples.

RNA sequencing

MHCC97-H cells were digested while adjusting to a cell density of (3×10^5)/mL and subsequently inoculated in 6-well plates containing 2 mL of cell suspension each well. The cells were incubated in a DMEM medium for 24 h. Blank control and test groups ($40 \mu\text{M/L}$) were established with three replicates of each sample, and cells were collected after 24 h. The Trizol technique was used to extract RNA from the interfering cells and tumor tissue, and the concentration and purity were assessed. Transcriptome sequencing was performed by Sangon Biotech (Shanghai) using the Illumina platform.

Western-blot analysis

MHCC97-H and Huh7 cells were grouped and treated for 48 h. Lysis buffer, PSME, and protein phosphatase inhibitor (100:1:1) were added to extract protein. The protein concentration was assessed using the BCA kit, followed by the addition of protein loading buffer, and the protein was boiled at 100°C for 10 min. We isolated the proteins using 12% SDS-PAGE. Proteins were subsequently electrophoresed in the gel. The proteins were transferred from the gel to a PVDF membrane upon completion of electrophoresis. The membranes were then incubated in primary (4°C , 8 h) and secondary antibodies (room temperature, 1 h), respectively. The bands' images were scan with chemiluminescence system (Bio-rad ChemiDoc MP).

Bioinformatics analysis for MAPK signaling pathway in HCC

To validate the MAPK related genes expression and their roles in HCC, we utilized the Cancer Genome Atlas (TCGA) database for analysis. The predictive impact of differentially expressed genes was evaluated using Kaplan–Meier analysis conducted in R language with the “survival” package. And $P < 0.05$ was considered significant.

Enrolled patients

To explore the potential relationship between ATO and the prognosis of HCC patients. The data of patients who underwent surgical resection for HCC at our institution between 2012 and 2018 was retrospectively evaluated. The identification of primary HCC was established using the Chinese Guidelines for the Management of Primary Liver Cancer²¹. Patient inclusion criteria were as follows: (I) patients of all genders, aged 18 to 75 years; (II) postoperative pathologically confirmed HCC; and (III) preoperative evaluation to confirm the feasibility of resection of HCC. Exclusion criteria included (I) secondary HCC, (II) early HCC intervention, such as transcatheter arterial embolization, radiofrequency ablation, or portal vein embolization, (III) HCC rupture and hemorrhage, (IV) loss following surgery to follow-up, (V) nonradical resection, and (VI) follow-up of less than 6 months. This retrospective chart review study involving human participants was in accordance with the ethical standards of the institutional and national research committee and with the 1964 Helsinki Declaration and its later amendments or comparable ethical standards. This study was approved by the Ethics Committee of the First Affiliated Hospital of Guangxi Medical University (No. 2022-KY-E-030). Individual consent for this retrospective analysis was waived.

Ethical approval

This study was approved by the Ethics Committee of the First Affiliated Hospital of Guangxi Medical University (Approval No. 2022-KY-E-030). We hereby confirm that: All experimental protocols were approved by the named institutional committee, namely the Ethics Committee of the First Affiliated Hospital of Guangxi Medical University. All methods were carried out in strict accordance with relevant guidelines and regulations governing experiments on live vertebrates. All methods reported in this manuscript adhere to the ARRIVE guidelines, ensuring comprehensive and transparent reporting of animal research.

Statistical analysis

The data analysis was conducted using the R software and Graph Pad Prism 8. Data are presented as mean \pm standard deviation (SD). The data were subjected to statistical analysis using Student's t-test, one-way or two-way ANOVA as appropriate, followed by post-hoc tests for multiple comparisons. With a significance level set at $P < 0.05$.

Results

In vitro experiments

We firstly used HCC cell lines MHCC97-H and Huh7 as the subjects and selected different concentrations of ATO for the intervention. The results inhibitory effect of ATO increasing while increasing ATO concentrations,

and the proliferation capacity of ATO-intervened HCC cells was significantly reduced compared to normal growing cells at different time points, showing concentration and time dependence (Fig. 1A, B). We set up blank control (CK), low concentration (10 $\mu\text{mol/L}$, L), medium concentration (20 $\mu\text{mol/L}$, M) and high concentration (40 $\mu\text{mol/L}$, H) groups for subsequent experiments based on the inhibitory effect of ATO on HCC cells. Next, we investigated the impact of ATO on the functionality of HCC cells. The HCC migration and invasion ability were found to be greatly decreased with increasing ATO concentration, as demonstrated by the Transwell Assay (Fig. 1C–G). Cell cycle assays demonstrated a substantial augmentation in the G1 phase accompanied by a significant shortening of (S+G2) in cells treated with all concentrations of ATO compared to normal growth HCC cells, consistent in MHCC97-H and Huh7 cell lines. These results revealed that ATO can induced G1 phase arrest (Fig. 1H–J).

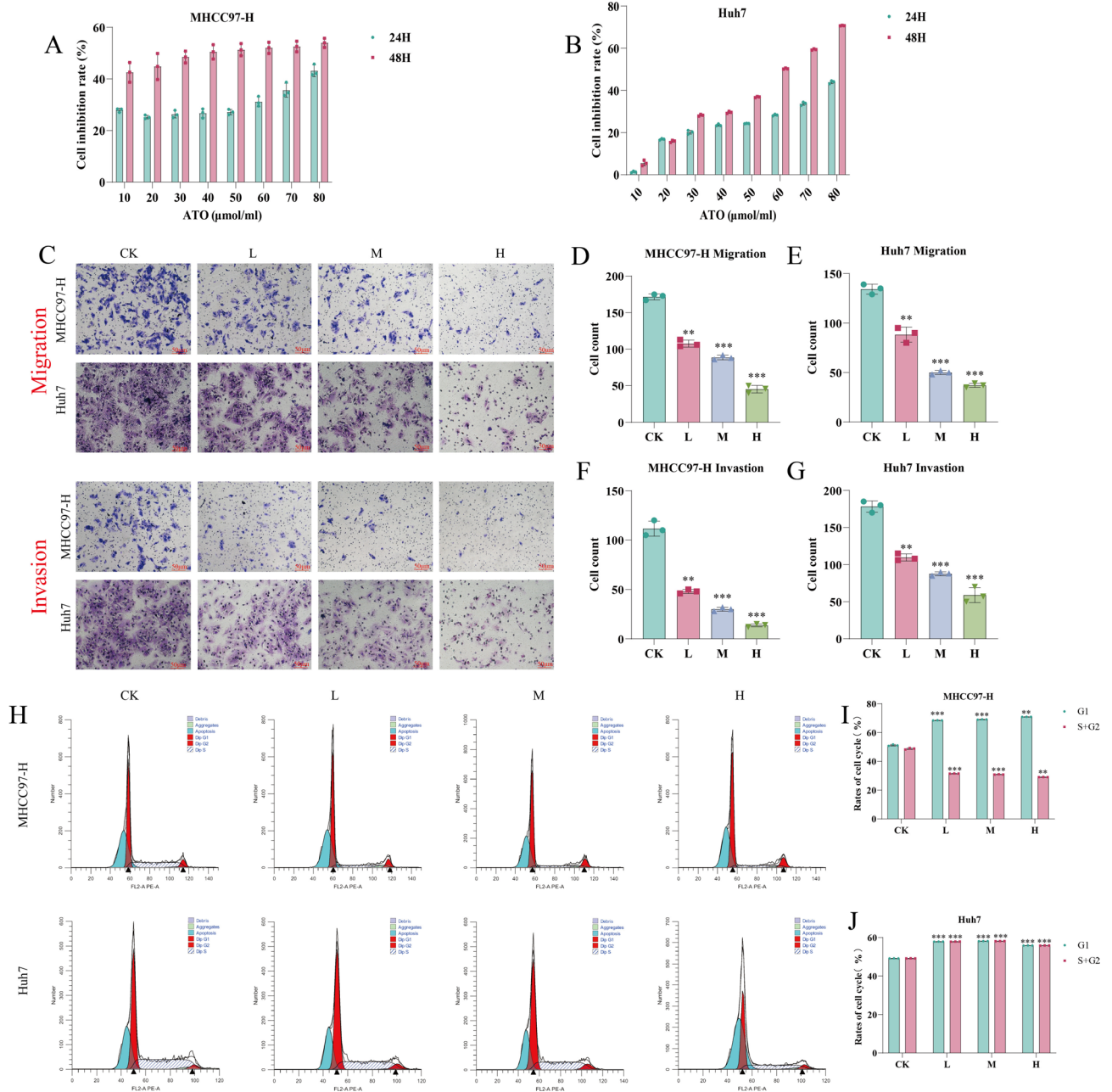


Fig. 1. Effect of ATO on proliferation, migration, invasion and cycle of hepatocellular carcinoma cell lines. (A, B) Effect of different concentrations of ATO on proliferation of hepatocellular carcinoma cell line MHCC97-H, Huh7; (C–E) Effect of different concentrations of ATO on migration of hepatocellular carcinoma cell line MHCC97-H (D), Huh7 (E); (C, F, G) Effect of different concentrations of ATO on invasion of hepatocellular carcinoma cell line MHCC97-H (F), Huh7 (G); (H–J) Effect of different concentrations of ATO on cell cycle of hepatocellular carcinoma cell line MHCC97-H (I), Huh7 (J). CK, Blank control group. Compared with control group * $P < 0.05$, ** $P < 0.01$, *** $P < 0.001$.

Effect of ATO on MAPK signaling pathway in HCC cells

To investigate the mechanism underlying the effect of ATO on HCC cells, we collected normal control and high concentration intervention HCC cells for RNA sequencing. Our screening identified 2264 differentially expressed genes, of which 832 genes were significantly up-regulated and 1432 significantly down-regulated, indicating that ATO significantly impacted the transcriptome expression of HCC cells (Fig. 2A). GO analysis showed that differentially expressed genes were mainly associated with lipid metabolism, regulation of signaling, blood vessel development and morphogenesis, cell proliferation, and cardiovascular system. The results of KEGG analysis indicated the functions of the differentially expressed genes are enriched in regulation of lipolysis in adipocyte, MAPK signaling, PI3K-AKT signaling, P53 signaling, and VEGF signaling pathways. We found that KOG (euKaryotic Ortholog Groups) analysis was enriched in functional clusters of lipid metabolism and cell cycle, such as lipid transport and metabolism, secondary metabolites biosynthesis and cell cycle control (Fig. 2B–D). Western blot analysis showed ATO decreased the expression of p-RAF1, p-MEK, p-ERK, p-P38, and p-JNK in vitro compared to controls, confirming ATO may mediate HCC cell function through the MAPK signaling pathway (Fig. 2E–F).

Effect of ATO on tumor growth in an animal model of HCC xenografts

To investigate the impact of ATO on tumors in vivo, we created a MHCC97-H HCC animal model and added a high-fat diet group to it. The success rate of mouse liver cancer xenograft model was 100% in immunodeficient BALB/c-nu/nu mice. In contrast to the control group, ATO-treated group did not exhibit a significantly decrease but rather increased in the tumor size; in terms of body weight, ATO treatment resulted in a reduction in the body weight of the mice (Fig. 3A–C). High-throughput sequencing of tumor tissues enriched the MAPK pathway in the normal diet group compared to cellular sequencing, which was consistent with the cellular results, while the pathway was not enriched in the high-fat diet group (Fig. 3D–K). Based on these data, lower doses of ATO were neither found to inhibit tumor growth in vivo nor were they beneficial to those who ate high-fat diets. Nevertheless, a high-fat diet increased the risk of developing hepatocellular carcinoma.

Effect of ATO on lipid metabolism indexes

The development of hepatocellular carcinogenesis is frequently accompanied by chronic inflammation. We also analyzed metabolic phenotypes associated with ATO intervention and different diet serum from mice to reveal metabolic phenotypes. Serum assays indicated that ATO treatment and a high-fat diet could reduce serum IL-10 levels and promote the release of IL-22. Using ATO alone or in conjunction with a high-fat diet reduced IL-23 release in the normal diet group, while using ATO increased IL-23 serum levels in high-fat diet group. In addition, the measurement of lipid-related indicators TC, TG, HDL-C, and LDL-C laterally confirmed the validity of our model (Fig. 4).

Expression levels of key genes in MAPK signaling pathway and their prognostic role in HCC

Comparing with healthy individuals most of the MAPK signaling pathway key genes were significantly overexpressed in HCC (Fig. 5), which results predicted that this high activation state of MAPK in HCC promotes the development of HCC. Overexpression of BRAF, DAB2, HRAS, MAP2K2, MAP3K4, MAPK3, MAPK7, MAPK13 and RAFFS1 could lead to poor prognosis of HCC (Fig. 6).

Association between ATO use and HCC prognosis

A total of 19 patients were retrieved who were regularly taking ATO preoperatively (Tables 1 and 2), and survival analysis showed that patients taking atorvastatin had better RFS ($P=0.037$) and marginal better OS ($P=0.062$) (Fig. 7A–B). We further used propensity score matching to eliminate the effect of the inclusion variable, and HCC patients who taking atorvastatin were matched 1:3 with those not taking ATO having better OS ($P=0.03$) after matching, while RFS ($P=0.11$) was inconsistent with OS (Fig. 7C–D). Given the small sample size and retrospective nature, these data suggest a potential benefit of ATO for HCC patients, which requires validation in larger, prospective studies.

Discussion

The primary approach for patients with early-stage HCC and those with a sufficient hepatic reserve is to undergo surgical resection. Despite this, postoperative recurrence remains one of the greatest challenges today. Five years after surgery, the cumulative recurrence rate has been greater than 50%. In addition to its antitumor properties, atorvastatin administration can elevate the risk of HCC. This study contradicts a study showing statins reduce tumorigenesis and improve prognosis among cancer patients. After in vivo/vitro experiments, this study confirms whether ATO is an antitumor agent or whether it promotes the development of HCC. We found that ATO may inhibit the occurrence and progression of liver cancer through the MAPK pathway (Fig. 8).

The results of in vitro experiments demonstrated that atorvastatin effectively suppressed the proliferation, migration, and invasion of HCC cells and also exerting regulatory effects on the cell cycle. Functional enrichment of mRNA sequencing showed that atorvastatin could act on MAPK signaling pathway in the experimental group. WB validation results showed a reduction in the levels of p-MEK, p-RAF1, p-P38, p-ERK, and p-JNK proteins. The MAPK signaling pathway was first identified as an oncogene in the 1970s and 1980s by sarcoma viruses²². The successive discovered of key molecules in the MAPK signaling pathways, including RAF, ERK, and MEK, has been facilitated by extensive research on viral oncogenes^{23–28}.

Further studies on the major molecules of MAPK pathway resulted in the identification of RAF as the upstream kinase of MEK and the initial direct effector of Ras in 1992 and 1993, respectively^{29,30}. Subsequent studies found high MAPK activity in more than 85% of tumors, according to the MAPK pathway crucial regulatory role in cell regulation. Its activity was regulated mainly directly through upstream genes and signaling

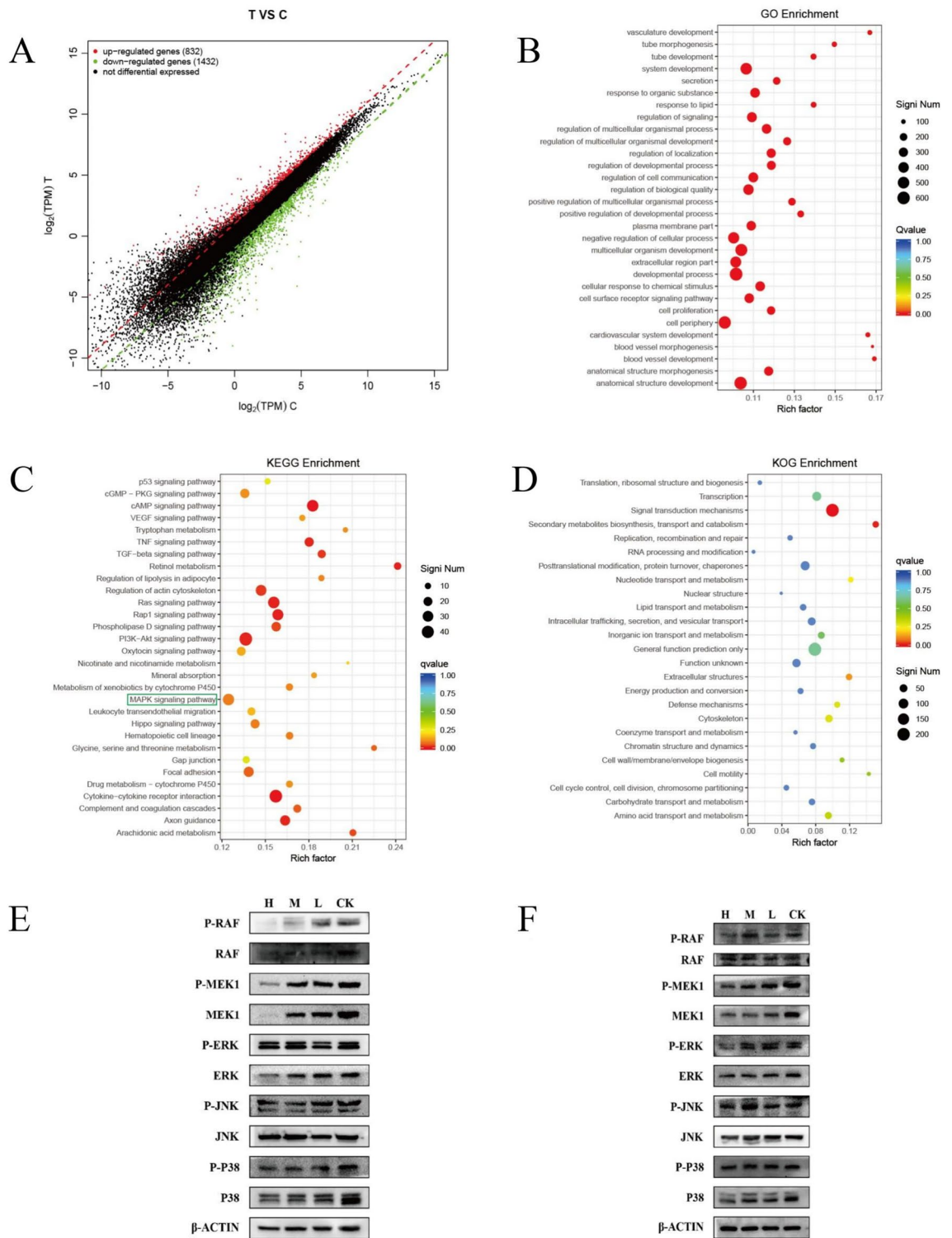


Fig. 2. Effect of ATO on MAPK signaling pathway in HCC cells. **(A)** Volcano map of differentially expressed genes. **(B–D)** GO **(B)**, KEGG **(C)**, KGO **(D)** enrichment analysis of differentially expressed genes. **(E, F)** Expression of key MAPK proteins in hepatoma cell line MHCC97-H and Huh7 with different concentrations of ATO intervention. GO, Gene Ontology. KEGG, Kyoto Encyclopedia of Genes and Genomes. KGO, euKaryotic Ortholog Groups.

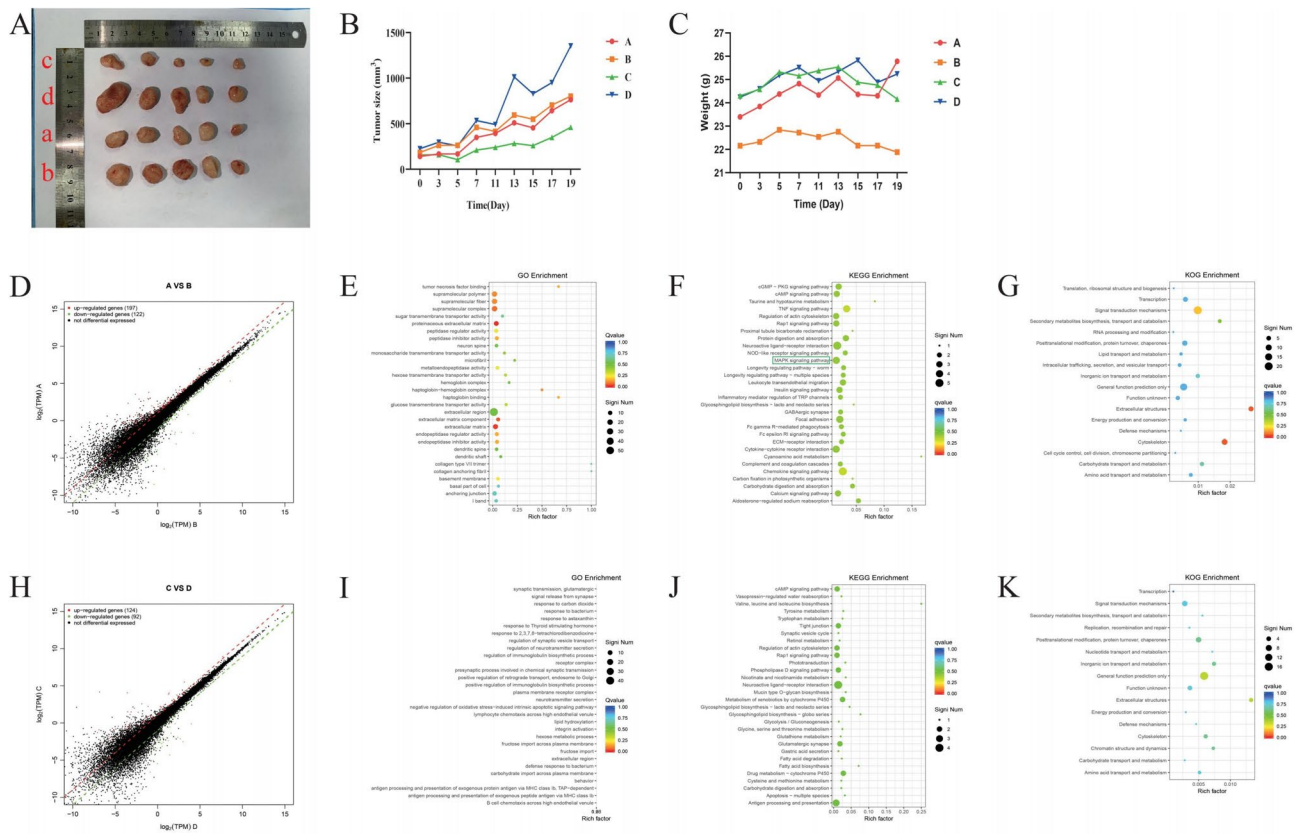


Fig. 3. Effect of ATO on tumor growth in hepatocellular carcinoma xenograft animal model. **(A)**, Tumor tissues of mice in different concentrations of ATO treatment groups. **(B)** Tumor volume change curves. **(C)** Body weight curves of mice. groups A and B are normal diet, groups C and D are high-fat diet, and groups B and D are ATO-treated groups. **(D–G)** Tumor GO, KEGG and KGO analysis of ATO-treated mice in the normal diet group. **(H–K)** Tumor GO, KEGG and KGO analysis of ATO-treated mice in the high-fat diet group. groups a and b were normal diet, groups c and d were high-fat diet, and b and d were ATO-treated groups. * $P < 0.05$, ** $P < 0.01$, *** $P < 0.001$.

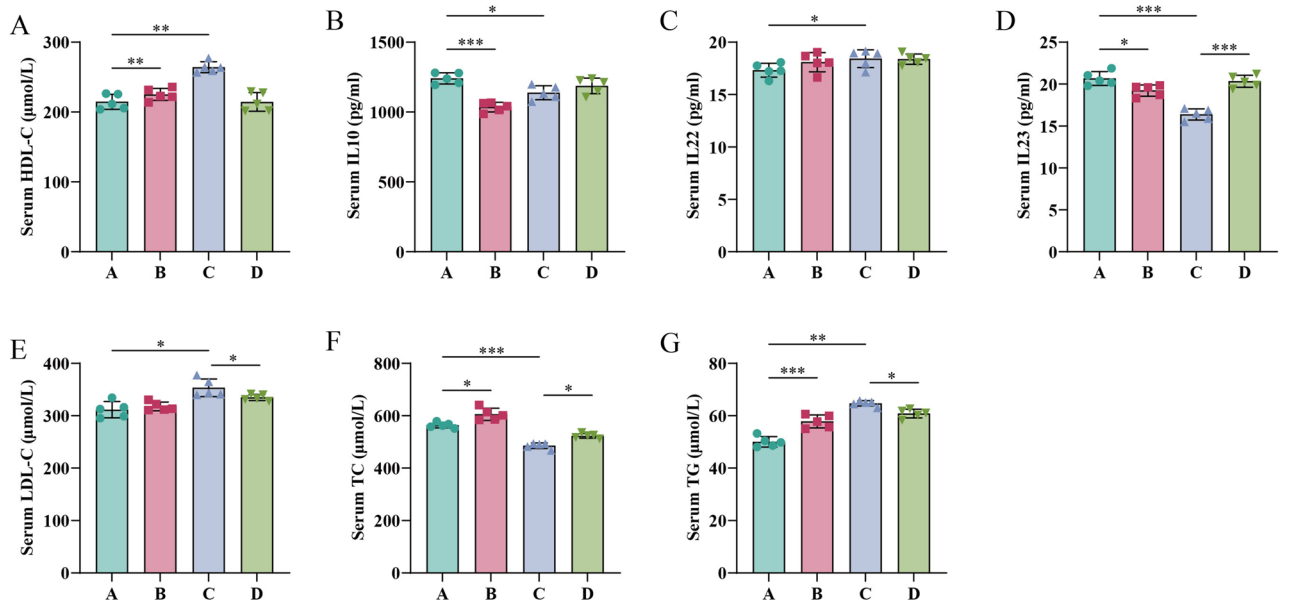


Fig. 4. Metabolic analysis of ATO treated mice. **(A)** HDL-C. **(B)** IL-10. **(C)** IL-22. **(D)** IL-23. **(E)** LDL-C. **(F)** TC. **(G)** TG. * $P < 0.05$, ** $P < 0.01$, *** $P < 0.001$.

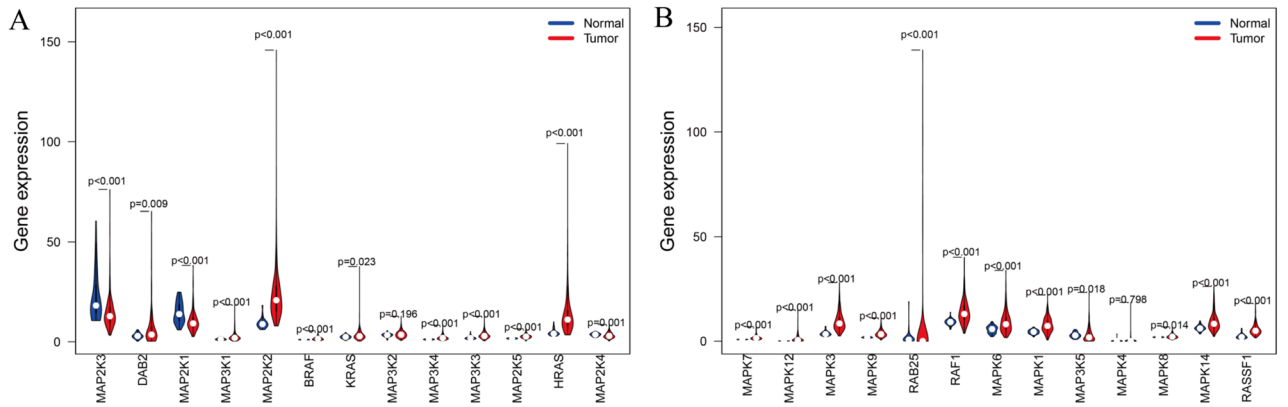


Fig. 5. Expression levels of key genes in MAPK signaling pathway.

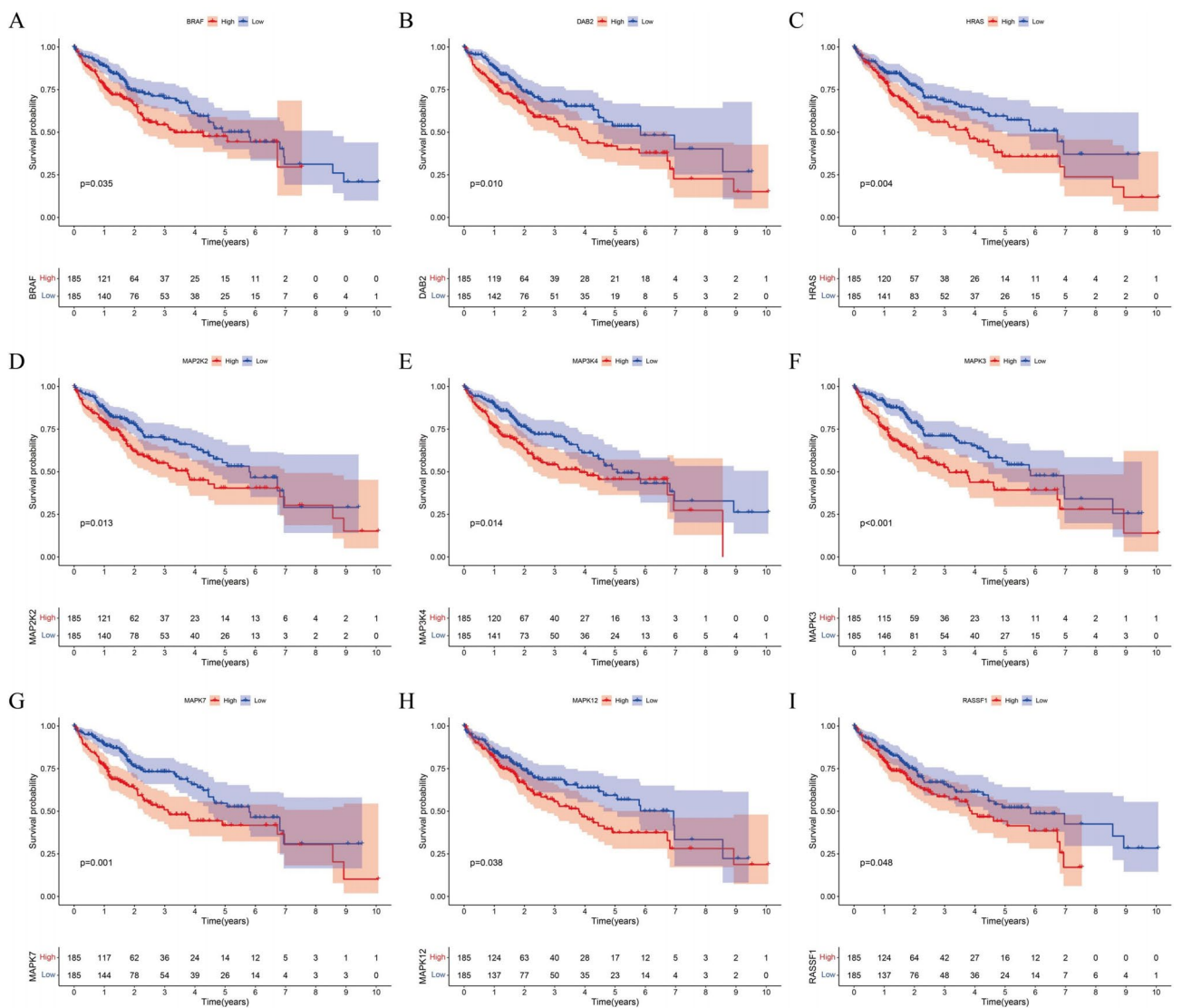


Fig. 6. Prognostic analysis of key genes in MAPK signaling pathway. (A) BRAF. (B) DAB2. (C) HRAS. (D) MAP2K2. (E) MAP3K4. (F) MAPK3. (G) MAPK7. (H) MAPK13. (I) RASSF1.

Variables	Value	OS				RFS			
		N	Events	HR(95%CI)	P	N	Events	HR (95%CI)	P
ATO	No	1451	328	1		1451	452	1	
	Yes	19	1	0.19(0.03, 1.34)	0.062	19	2	0.26(0.06, 1.02)	0.037
Age	< 60	1219	279	1		1219	387	1	
	≥ 60	251	50	0.81(0.6, 1.1)	0.174	251	67	0.8(0.62, 1.04)	0.098
Gender	Male	232	41	1		232	51	1	
	Female	1238	288	1.32(0.95, 1.84)	0.092	1238	403	1.53(1.14, 2.05)	0.004
BMI	< 24	989	223	1		989	305	1	
	≥ 24	481	106	0.94(0.75, 1.19)	0.629	481	149	0.97(0.8, 1.18)	0.744
Smoking	No	950	216	1		950	284	1	
	Yes	520	113	0.99(0.79, 1.24)	0.918	520	170	1.14(0.94, 1.38)	0.182
Alcohol	No	1000	241	1		1000	317	1	
	Yes	470	88	0.8(0.63, 1.03)	0.08	470	137	0.94(0.77, 1.14)	0.515
Diabetes	No	1362	299	1		1362	420	1	
	Yes	108	30	1.29(0.89, 1.88)	0.176	108	34	1.04(0.73, 1.48)	0.815
Hypertension	No	1327	307	1		1327	425	1	
	Yes	143	22	0.64(0.41, 0.98)	0.039	143	29	0.59(0.4, 0.86)	0.005
AFP	< 400	930	187	1		930	278	1	
	≥ 400	540	142	1.53(1.23, 1.9)	<0.001	540	176	1.28(1.06, 1.55)	0.01
BCLC stage	0 or A	1161	227	1		1161	341	1	
	B or C	309	102	2.71(2.14, 3.43)	<0.001	309	113	1.98(1.6, 2.46)	<0.001
Child pugh	A	1412	304	1		1412	432	1	
	B	58	25	2.57(1.71, 3.86)	<0.001	58	22	1.74(1.14, 2.68)	0.01
Cirrhosis	No	775	153	1		775	235	1	
	Yes	695	176	1.28(1.03, 1.59)	0.023	695	219	1.05(0.88, 1.27)	0.578
Clonorchissinensis	No	1313	296	1		1313	399	1	
	Yes	157	33	0.85(0.59, 1.21)	0.362	157	55	1.1(0.83, 1.46)	0.506
Venous tumor thrombus	No	1285	265	1		1285	399	1	
	Yes	185	64	3.31(2.51, 4.38)	<0.001	185	55	1.77(1.33, 2.36)	<0.001
Tumor number	1	1275	269	1		1275	367	1	
	≥ 1	195	60	1.74(1.31, 2.3)	<0.001	195	87	2(1.58, 2.53)	<0.001
Tumor size max	< 5 cm	766	124	1		766	217	1	
	≥ 5 cm	704	205	2.29(1.83, 2.86)	<0.001	704	237	1.53(1.27, 1.84)	<0.001
Hepatitis	No	232	47	1		232	59	1	
	HBV	1220	279	1.14(0.84, 1.56)	0.395	1220	388	1.29(0.98, 1.7)	0.068
	HCV	18	3	0.66(0.21, 2.13)	0.487	18	7	1.42(0.65, 3.12)	0.377
MVI	No	967	169	1		967	270	1	
	Yes	503	160	2.35(1.89, 2.92)	<0.001	503	184	1.72(1.43, 2.08)	<0.001
Duration of operation	< 240	814	175	1		814	224	1	
	≥ 240	656	154	1.13(0.91, 1.4)	0.274	656	230	1.35(1.12, 1.62)	0.001
Bleeding	< 400	829	140	1		829	231	1	
	≥ 400	641	189	1.93(1.55, 2.4)	<0.001	641	223	1.41(1.17, 1.69)	<0.001
Surgical approach	Open surgery	1186	289	1		1186	392	1	
	Laparoscope	284	40	0.61(0.44, 0.85)	0.003	284	62	0.65(0.5, 0.85)	0.002
Radical resection	Yes	905	161	1		905	251	1	
	No	565	168	2.02(1.63, 2.51)	<0.001	565	203	1.6(1.33, 1.93)	<0.001

Table 1. Single factor analysis before matching analysis. ATO, Atorvastatin. BMI, Body mass index. AFP, alpha-fetoprotein. BCLC, Barcelona clinic liver cancer stage. MVI, Microvascular Invasion. HBV, Hepatitis B Virus. HCV, Hepatitis C Virus. HR, calculated by Cox proportional hazards regression model. *P*, calculated by log-rank test.

pathway components like RTKs, Ras, and BRAF activity or indirectly through non-Ras- or RAF-dependent activation pathways^{31–33}. Consequently, we speculate that a highly active MAPK pathway can promote cancer development. Abnormal mutations of crucial elements in the MAPK pathway, including Ras, RAF, MEK, and ERK can affect the development of hepatocellular carcinoma^{34–37}. High activity of the above key components is generally used as cancer-promoting factors in HCC. Even so, factors that cause MAPK to become highly active

Variables	Value	OS				RFS			
		N	Events	HR(95%CI)	P	N	Events	HR(95%CI)	P
ATO	No	57	15	1		57	14	1	
	Yes	19	1	0.15(0.02, 1.1)	0.03	19	2	0.32(0.07, 1.41)	0.112
Age	< 60	47	10	1		47	11	1	
	≥ 60	29	6	0.81(0.29, 2.23)	0.682	29	5	0.62(0.22, 1.8)	0.38
Gender	Male	14	1	1		14	2	1	
	Female	62	15	3.21(0.42, 24.32)	0.233	62	14	1.47(0.33, 6.49)	0.607
BMI	< 24	40	9	1		40	8	1	
	≥ 24	36	7	0.81(0.3, 2.18)	0.68	36	8	1.05(0.39, 2.79)	0.929
Smoking	No	56	14	1		56	11	1	
	Yes	20	2	0.4(0.09, 1.76)	0.209	20	5	1.29(0.45, 3.72)	0.638
Alcohol	No	56	15	1		56	12	1	
	Yes	20	1	0.17(0.02, 1.26)	0.048	20	4	0.83(0.27, 2.58)	0.745
Diabetes	No	42	10	1		42	8	1	
	Yes	34	6	0.76(0.28, 2.09)	0.594	34	8	1.26(0.47, 3.37)	0.639
Hypertension	No	39	13	1		39	11	1	
	Yes	37	3	0.2(0.06, 0.69)	0.005	37	5	0.39(0.14, 1.13)	0.073
AFP	< 400	52	12	1		52	9	1	
	≥ 400	24	4	0.67(0.21, 2.08)	0.482	24	7	1.71(0.63, 4.63)	0.286
BCLC stage	0 or A	62	10	1		62	12	1	
	B or C	14	6	4.27(1.46, 12.5)	0.004	14	4	2.38(0.73, 7.71)	0.136
Child pugh	A	71	13	1		71	15	1	
	B	5	3	7.48(2.04, 27.48)	<0.001	5	1	1.78(0.23, 13.75)	0.576
Cirrhosis	No	58	9	1		58	13	1	
	Yes	18	7	3.18(1.18, 8.58)	0.016	18	3	0.9(0.26, 3.19)	0.876
Clonorchissinensis	No	66	15	1		66	14	1	
	Yes	10	1	0.51(0.07, 3.9)	0.513	10	2	1.04(0.24, 4.58)	0.961
Venous tumor thrombus	No	66	12	1		66	13	1	
	Yes	10	4	3.73(1.14, 12.2)	0.019	10	3	2.72(0.74, 10.02)	0.118
Tumor number	1	70	13	1		70	15	1	
	≥ 1	6	3	3.66(1.01, 13.21)	0.034	6	1	0.98(0.13, 7.54)	0.987
Tumor size max	< 5 cm	35	7	1		35	3	1	
	≥ 5 cm	41	9	1.42(0.52, 3.86)	0.489	41	13	4.84(1.37, 17.19)	0.007
Hepatitis	No	22	4	1		22	6	1	
	HBV	54	12	1.35(0.44, 4.19)	0.601	54	10	0.7(0.25, 1.92)	0.481
MVI	No	50	11	1		50	8	1	
	Yes	26	5	1.11(0.38, 3.2)	0.852	26	8	2.4(0.9, 6.44)	0.073
Duration of operation	< 240	37	6	1		37	6	1	
	≥ 240	39	10	1.78(0.65, 4.92)	0.257	39	10	1.74(0.63, 4.79)	0.282
Bleeding	< 400	43	6	1		43	9	1	
	≥ 400	33	10	2.31(0.84, 6.37)	0.095	33	7	1.05(0.39, 2.83)	0.917
Surgical approach	Open surgery	59	12	1		59	14	1	
	Laparoscope	17	4	1.13(0.37, 3.52)	0.828	17	2	0.5(0.11, 2.18)	0.343
Radical resection	Yes	51	9	1		51	7	1	
	No	25	7	1.52(0.56, 4.09)	0.407	25	9	2.62(0.98, 7.06)	0.047

Table 2. Single factor analysis after matching analysis. ATO, Atorvastatin. BMI, Body mass index. AFP, alpha-fetoprotein. BCLC, Barcelona clinic liver cancer stage. MVI, Microvascular Invasion. HBV, Hepatitis B Virus. HR, calculated by Cox proportional hazards regression model. *P*, calculated by log-rank test.

are crucial to the development of HCC and the known cytokines. MAPK pathway activity should be studied in depth in relation to various factors, including energy substance metabolism and intestinal flora composition. Alterations in MAPK pathway genes can lead to abnormal MAPK signaling pathway conduction. Different mutations in MAPK pathway genes may result in very different outcomes. This study suggested ATO may play a role in the regulation of HCC via affecting the MAPK signaling pathway at the cellular level, which was verified in animals with altered dietary factors, and finally further confirmed in combination with clinical patient data.

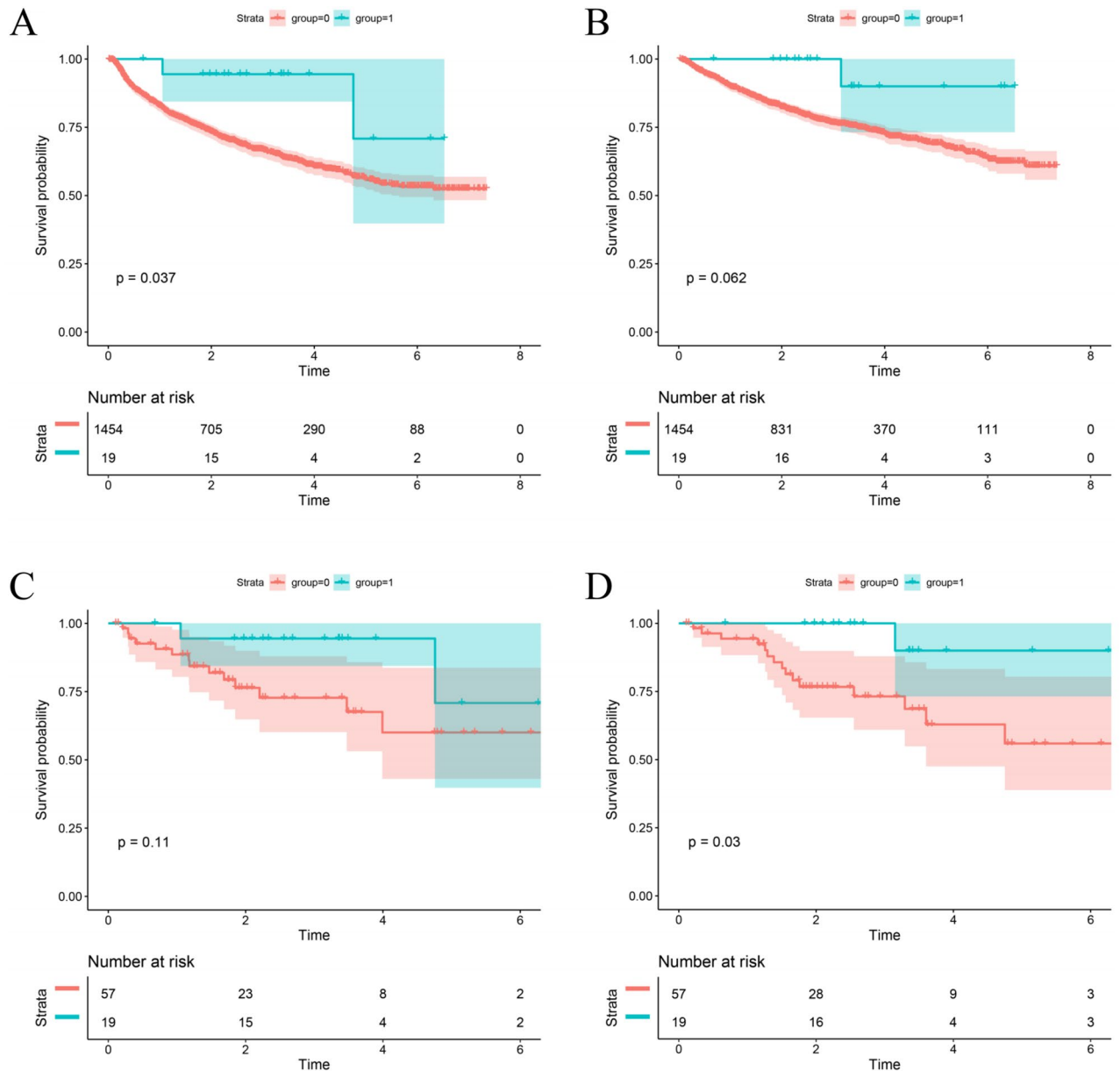


Fig. 7. Prognostic analysis of HCC patients taking ATO. (A–B) Pre-match RFS and OS analysis. (C–D) Post-matching RFS and OS analysis. group = 0, HCC patients not taking ATO. group = 1, HCC patients taking ATO.

Aberrant MAPK pathway transduction not only has a significant impact on HCC development, but it may also lead to poor drug efficacy in the treatment of HCC, as inhibition of its activity can increase drug sensitivity to HCC^{38,39}. Due to the vital role of MAPK pathway in cancer development, many studies have been conducted to design targeted drugs for key factors of MAPK pathway^{40–42}. In mammals, MAPK regulates cell biological behaviors through extracellular signaling MAPK pathways. In addition to classical MAPK/MEK pathway activation pathway also includes signaling pathways such as C-Jun and P38. Therefore, MAPK pathway significantly impacts occurrence, development, treatment responsiveness, and prognosis of HCC. The mechanism leading to high activity in HCC remains incompletely understood. The study of in-vitro experiments demonstrated that ATO inhibited the expression of p-RAF1, p-MEK, p-ERK, p-P38, and p-JNK proteins in HCC cells and in vitro cells confirmed that ATO may inhibit HCC development through MAPK signaling pathway. We consider that it is related to the patient's long-term use of ATO, which may reduce the inflammatory response of the liver and bile in addition to lowering blood lipids, but whether it can prevent HCC recurrence and metastasis remains to be investigated.

A statin is an inhibitor of HMG-CoA reductase used to treat dyslipidemia and prevent cardiovascular events. Research has demonstrated lipids have a crucial regulatory function in the development of cancers, including pancreatic, breast, and prostate cancers^{11–13}. Henceforth, we speculate that atorvastatin may regulate lipid metabolism and affect the development of HCC. Hence, we compared the progression of HCC in an animal

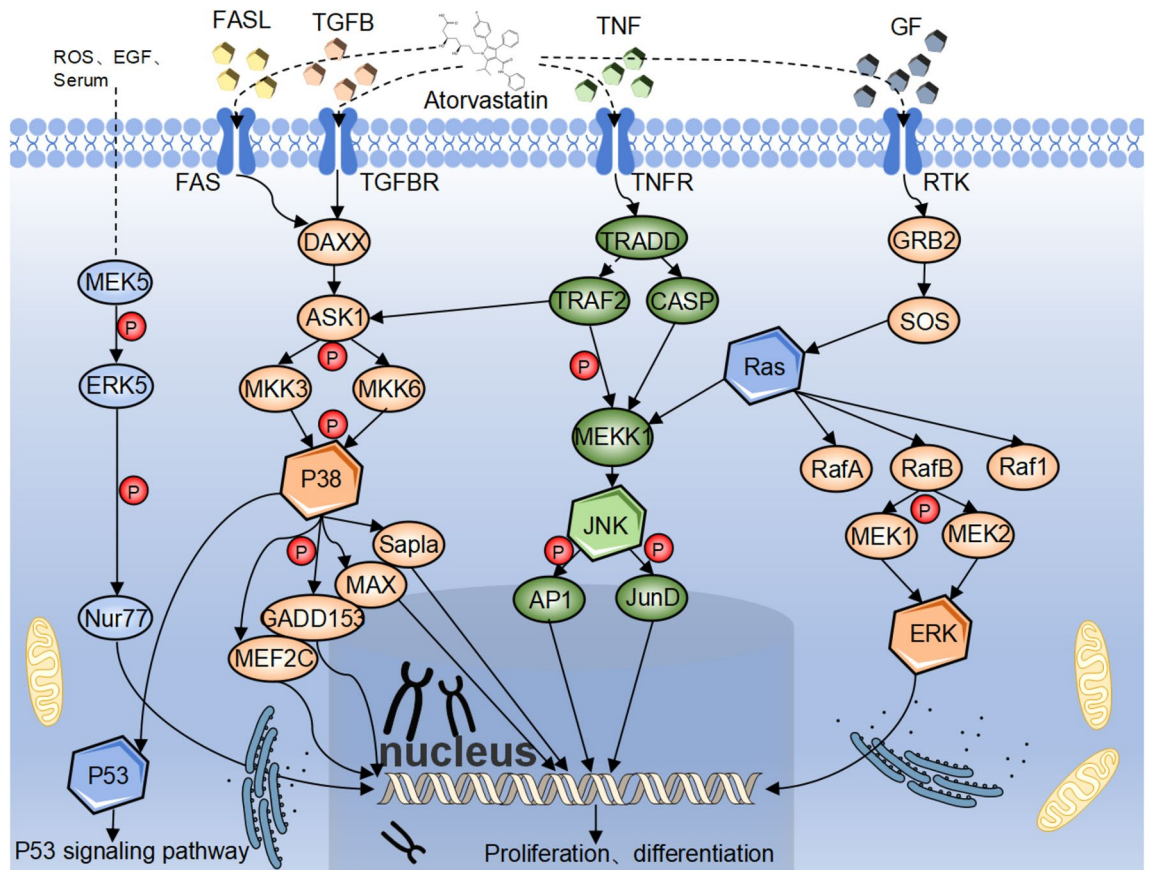


Fig. 8. ATO acts through MAPK pathway with in vivo and in vitro mechanism.

model subjected to a high-fat diet and a normal diet, respectively, and intervened with ATO. In vitro showed that a high-fat diet promoted the development of HCC, while ATO had no antitumor activity in vivo. We consider that it is related to the dose of drug administered and the mode of tumorigenesis. The subcutaneous xenograft model in immunodeficient mice, while useful for initial tumor growth studies, does not fully recapitulate the complex tumor microenvironment (TME), including immune cell interactions and the specific liver TME shaped by chronic liver disease, steatosis, or fibrosis. The high-fat diet-induced metabolic changes in this model may not be sufficient to override the strong oncogenic drive of the subcutaneously implanted human cancer cells or to render them sensitive to the antiproliferative effects of ATO at the dose used. Future studies should consider using immunocompetent, genetically engineered, or carcinogen-induced models that better mimic the pathogenesis of steatohepatitis-associated HCC. At the same time, ATO, as a lipid-lowering drug, may be stimulated by a high-fat diet. The observed cytokine changes are intriguing. IL-22 can have dual roles in cancer, often associated with tissue repair but also potentially promoting proliferation in established tumors. The significant increase in IL-23 in the HFD + ATO group (Group D) compared to HFD alone (Group C) is notable, as IL-23 is a key inflammatory cytokine implicated in tumorigenesis and immune suppression. The interplay between ATO, diet, and the immune response within the TME is complex and warrants further investigation, including direct measurement of intratumoral lipid metabolites and immune cell infiltration. Through retrospective analysis of clinical cases, we found that atorvastatin showed a positive effect on the prognosis of HCC patients. However, it is important to note that although atorvastatin showed potential benefits, our study may have limitations in the length of the intervention, which may have resulted in significant efficacy gains not yet observed. Therefore, future studies may require longer follow-up and more refined intervention strategies to more fully assess the potential of atorvastatin to improve outcomes in HCC patients. Furthermore, the retrospective clinical analysis, though suggestive of a benefit, is limited by the small sample size ($n = 19$ ATO users) and lack of detailed data on ATO dosage, duration, and patient adherence. As the vast majority of patients in this retrospective clinical database did not have their preoperative lipid indicators systematically tested, effective correction analysis could not be conducted. The observed survival advantage could potentially be influenced by baseline lipid profiles or other confounding factors not fully accounted for by propensity score matching. Larger-scale, prospective studies with detailed drug exposure and metabolic data are needed to confirm these preliminary findings and establish causality.

Conclusion

ATO has significant anti-hepatocarcinogenic activity *in vitro* by inhibiting the MAPK pathway. Our study found that high-fat diets could promote HCC development in animal models. However, in our subcutaneous xenograft model, animal models showed no antitumor activity for ATO, highlighting the context-dependent nature of its effects and the limitations of the model used. Thus, further research is required to investigate the effects of gut microbiota and metabolites on HCC development under a high-lipid diet and ATO treatment conditions. Interestingly, retrospective clinical data suggest ATO has the potential to enhance the prognosis of HCC patients, although this requires validation in larger prospective cohorts.

Data availability

All data can be obtained from <https://data.mendeley.com/preview/7mn636j4pc?a=2b423c32-d722-40da-8c8a-f611ae02a95a> (<https://doi.org/10.17632/7mn636j4pc.1>), or contact hyf20190701@163.com.

Received: 12 March 2025; Accepted: 17 October 2025

Published online: 21 November 2025

References

- Kim, E. & Viatour, P. Hepatocellular carcinoma: Old friends and new tricks. *Exp. Mol. Med.* **52**(12), 1898–1907. <https://doi.org/10.1038/s12276-020-00527-1> (2020).
- Duran, S. & Jaquiss, R. Hepatocellular carcinoma. *N. Engl. J. Med.* **381**(1), e2. <https://doi.org/10.1056/NEJMc1906565> (2019).
- Yang, J. & Roberts, L. Hepatocellular carcinoma: A global view. *Nat. Rev. Gastroenterol. Hepatol.* **7**(8), 448–458. <https://doi.org/10.1038/nrgastro.2010.100> (2010).
- Younossi, Z. et al. The Economic and clinical burden of nonalcoholic fatty liver disease in the United States and Europe. *Hepatology* **64**(5), 1577–1586. <https://doi.org/10.1002/hep.28785> (2016).
- Rebouissou, S. & Nault, J. Advances in molecular classification and precision oncology in hepatocellular carcinoma. *J. Hepatol.* **72**(2), 215–229. <https://doi.org/10.1016/j.jhep.2019.08.017> (2020).
- Behary, J. et al. Gut microbiota impact on the peripheral immune response in non-alcoholic fatty liver disease related hepatocellular carcinoma. *Nat. Commun.* **12**(1), 187. <https://doi.org/10.1038/s41467-020-20422-7> (2021).
- Omata, M. et al. Asia-Pacific clinical practice guidelines on the management of hepatocellular carcinoma: A 2017 update. *Hep. Intl.* **11**(4), 317–370. <https://doi.org/10.1007/s12072-017-9799-9> (2017).
- Huang, A., Yang, X., Chung, W., Dennison, A. & Zhou, J. Targeted therapy for hepatocellular carcinoma. *Signal Transduct. Target. Ther.* **5**(1), 146. <https://doi.org/10.1038/s41392-020-00264-x> (2020).
- Pinter, M., Scheiner, B. & Peck-Radosavljevic, M. Immunotherapy for advanced hepatocellular carcinoma: A focus on special subgroups. *Gut* **70**(1), 204–214. <https://doi.org/10.1136/gutjnl-2020-321702> (2021).
- Bian, X. et al. Lipid metabolism and cancer. *J. Exp. Med.* **218**(1), e20201606. <https://doi.org/10.1084/jem.20201606> (2021).
- Nelson, E. The significance of cholesterol and its metabolite, 27-hydroxycholesterol in breast cancer. *Mol. Cell. Endocrinol.* **466**, 73–80. <https://doi.org/10.1016/j.mce.2017.09.021> (2018).
- Gao, L. et al. Cpi-613 rewires lipid metabolism to enhance pancreatic cancer apoptosis via the Ampk-Acc signaling. *J. Exp. Clin. Cancer Res. CR.* **39**(1), 73. <https://doi.org/10.1186/s13046-020-01579-x> (2020).
- Škara, L. et al. Prostate cancer-focus on cholesterol. *Cancers* **13**(18), 4696. <https://doi.org/10.3390/cancers13184696> (2021).
- Che, L. et al. Cholesterol biosynthesis supports the growth of hepatocarcinoma lesions depleted of fatty acid synthase in mice and humans. *Gut* **69**(1), 177–186. <https://doi.org/10.1136/gutjnl-2018-317581> (2020).
- Zhang, X. et al. Dietary cholesterol drives fatty liver-associated liver cancer by modulating gut microbiota and metabolites. *Gut* **70**(4), 761–774. <https://doi.org/10.1136/gutjnl-2019-319664> (2021).
- Zhou, F. & Sun, X. Cholesterol metabolism: A double-edged sword in hepatocellular carcinoma. *Front. Cell Dev. Biol.* **9**, 762828. <https://doi.org/10.3389/fcell.2021.762828> (2021).
- Nielsen, S., Nordestgaard, B. & Bojesen, S. Statin use and reduced cancer-related mortality. *N. Engl. J. Med.* **367**(19), 1792–1802. <https://doi.org/10.1056/NEJMoa1201735> (2012).
- Simon, T., Bonilla, H., Yan, P., Chung, R. & Butt, A. Atorvastatin and fluvastatin are associated with dose-dependent reductions in cirrhosis and hepatocellular carcinoma, among patients with hepatitis C virus: Results from erchives. *Hepatology* **64**(1), 47–57. <https://doi.org/10.1002/hep.28506> (2016).
- Islam, M., Poly, T., Walther, B., Yang, H. & Jack, L. Y. Statin use and the risk of hepatocellular carcinoma: A meta-analysis of observational studies. *Cancers* **12**(3), 671. <https://doi.org/10.3390/cancers12030671> (2020).
- Wang, S. et al. Atorvastatin-induced senescence of hepatocellular carcinoma is mediated by downregulation of Htert through the suppression of the Il-6/Stat3 pathway. *Cell Death Discov.* **6**, 17. <https://doi.org/10.1038/s41420-020-0252-9> (2020).
- Zhou, J. et al. Guidelines for the diagnosis and treatment of hepatocellular carcinoma (2019 edition). *Liver Cancer* **9**(6), 682–720. <https://doi.org/10.1159/000509424> (2020).
- Rapp, U. & Todaro, C. Generation of new mouse sarcoma viruses in cell culture. *Science* **201**(4358), 821–824. <https://doi.org/10.1126/science.210501> (1978).
- Bonner, T. et al. The human homologs of the Raf (Mil) oncogene are located on human chromosomes 3 and 4. *Science* **223**(4631), 71–74. <https://doi.org/10.1126/science.6691137> (1984).
- Ray, L. & Sturgill, T. Characterization of insulin-stimulated microtubule-associated protein kinase rapid isolation and stabilization of a novel serine/threonine kinase from 3t3-L1 cells. *J. Biol. Chem.* **263**(25), 12721–12727 (1988).
- Rossomando, A., Payne, D., Weber, M. & Sturgill, T. Evidence that Pp42, a major tyrosine kinase target protein, is a mitogen-activated serine/threonine protein kinase. *Proc. Natl. Acad. Sci. U.S.A.* **86**(18), 6940–6943. <https://doi.org/10.1073/pnas.86.18.6940> (1989).
- Ahn, N., Weiel, J., Chan, C. & Krebs, E. Identification of multiple epidermal growth factor-stimulated protein serine/threonine kinases from swiss 3t3 cells. *J. Biol. Chem.* **265**(20), 11487–11494 (1990).
- Boulton, T. et al. Erks: A family of protein-serine/threonine kinases that are activated and tyrosine phosphorylated in response to insulin and Ngf. *Cell* **65**(4), 663–675. [https://doi.org/10.1016/0092-8674\(91\)90098-j](https://doi.org/10.1016/0092-8674(91)90098-j) (1991).
- Crews, C. & Erikson, R. Purification of a murine protein-tyrosine/threonine kinase that phosphorylates and activates the Erk-1 gene product: Relationship to the fission yeast Byr1 gene product. *Proc. Natl. Acad. Sci. U.S.A.* **89**(17), 8205–8209. <https://doi.org/10.1073/pnas.89.17.8205> (1992).
- Rapp, U. et al. Structure and biological activity of V-Raf, a unique oncogene transduced by a retrovirus. *Proc. Natl. Acad. Sci. U.S.A.* **80**(14), 4218–4222. <https://doi.org/10.1073/pnas.80.14.4218> (1983).
- Moelling, K., Heimann, B., Beimpling, P., Rapp, U. & Sander, T. Serine- and threonine-specific protein kinase activities of purified Gag-Mil and Gag-Raf proteins. *Nature* **312**(5994), 558–561. <https://doi.org/10.1038/312558a0> (1984).

31. Xu, S. et al. Differential regulation of mitogen-activated protein/Erk kinase (Mek)1 and Mek2 and activation by a Ras-independent mechanism. *Mol. Endocrinol.* **11**(11), 1618–1625. <https://doi.org/10.1210/mend.11.11.0010> (1997).
32. Jun, S. et al. Paf-mediated Mapk signaling hyperactivation Via Lamtor3 induces pancreatic tumorigenesis. *Cell Rep.* **5**(2), 314–322. <https://doi.org/10.1016/j.celrep.2013.09.026> (2013).
33. Drost, M. et al. Loss of P53 induces cell proliferation via Ras-independent activation of the Raf/Mek/Erk signaling pathway. *Proc. Natl. Acad. Sci. U.S.A.* **111**(42), 15155–15160. <https://doi.org/10.1073/pnas.1417549111> (2014).
34. Delire, B. & Stärkel, P. The Ras/Mapk pathway and hepatocarcinoma: Pathogenesis and therapeutic implications. *Eur. J. Clin. Invest.* **45**(6), 609–623. <https://doi.org/10.1111/eci.12441> (2015).
35. Li, Q. et al. Hscs-derived comp drives hepatocellular carcinoma progression by activating Mek/Erk and Pi3k/Akt signaling pathways. *J. Exp. Clin. Cancer Res. CR.* **37**(1), 231. <https://doi.org/10.1186/s13046-018-0908-y> (2018).
36. Moon, H. & Ro, S. Mapk/Erk signaling pathway in hepatocellular carcinoma. *Cancers* **13**(12), 3026. <https://doi.org/10.3390/cancers13123026> (2021).
37. Rudalska, R. et al. Lxra activation and Raf inhibition trigger lethal lipotoxicity in liver cancer. *Nature Cancer* **2**(2), 201–217. <https://doi.org/10.1038/s43018-020-00168-3> (2021).
38. Li, Q. et al. Blocking Mapk/Erk pathway sensitizes hepatocellular carcinoma cells to temozolomide via downregulating Mgmt expression. *Ann. Transl. Med.* **8**(20), 1305. <https://doi.org/10.21037/atm-20-5478> (2020).
39. Xing, S., Chen, S., Yang, X. & Huang, W. Role of Mapk Activity in Pd-L1 Expression in Hepatocellular Carcinoma Cells. *J. BUON. Off. J. Balkan Union Oncol.* **25**(4), 1875–1882 (2020).
40. Athuluri-Divakar, S. et al. A small molecule Ras-mimetic disrupts Ras association with effector proteins to block signaling. *Cell* **165**(3), 643–655. <https://doi.org/10.1016/j.cell.2016.03.045> (2016).
41. Herrero, A. et al. Small molecule inhibition of Erk dimerization prevents tumorigenesis by Ras-Erk pathway oncogenes. *Cancer Cell* **28**(2), 170–182. <https://doi.org/10.1016/j.ccell.2015.07.001> (2015).
42. Sabesin, S. et al. Comparative evaluation of gastrointestinal intolerance produced by plain and tri-buffered aspirin tablets. *Am. J. Gastroenterol.* **83**(11), 1220–1225 (1988).

Acknowledgements

Thanks to the Animal Laboratory Center of Guangxi Medical University and the Cancer Genome Atlas database for support.

Author contributions

All authors participated in Writing—Original Draft Preparation. Yuhua Meng, Methodology and Formal Analysis. Linfang Mo, Investigation and Supervision. Tianyi Liang, Software and Validation. Shutian Mo, Resources, Data Curation and Visualization. Chuangye Han Conceptualization and Funding Acquisition. Yongfei He Writing—Review & Editing, Project Administration and Funding Acquisition.

Funding

This study was supported by the China Postdoctoral Science Foundation(2023M744020), National Natural Science Foundation of China (81560535, 81802874 and 81072321), Guangxi Medical and Health Appropriate Technology Development and Application Project (S2021100).

Declarations

Competing interests

The authors declare no competing interests.

Ethics approval

This study was approved by the Ethics Committee of the First Affiliated Hospital of Guangxi Medical University (Approval No. 2022-KY-E-030), confirming that a named institutional committee approved all experimental protocols. Relevant guidelines and regulations are carried out in all methods. Additionally, we confirm that all methods are reported following the ARRIVE guidelines.

Additional information

Supplementary Information The online version contains supplementary material available at <https://doi.org/10.1038/s41598-025-25040-1>.

Correspondence and requests for materials should be addressed to C.H. or Y.H.

Reprints and permissions information is available at www.nature.com/reprints.

Publisher's note Springer Nature remains neutral with regard to jurisdictional claims in published maps and institutional affiliations.

Open Access This article is licensed under a Creative Commons Attribution-NonCommercial-NoDerivatives 4.0 International License, which permits any non-commercial use, sharing, distribution and reproduction in any medium or format, as long as you give appropriate credit to the original author(s) and the source, provide a link to the Creative Commons licence, and indicate if you modified the licensed material. You do not have permission under this licence to share adapted material derived from this article or parts of it. The images or other third party material in this article are included in the article's Creative Commons licence, unless indicated otherwise in a credit line to the material. If material is not included in the article's Creative Commons licence and your intended use is not permitted by statutory regulation or exceeds the permitted use, you will need to obtain permission directly from the copyright holder. To view a copy of this licence, visit <http://creativecommons.org/licenses/by-nc-nd/4.0/>.

© The Author(s) 2025